FRICTION-INDUCED STRUCTURAL TRANSFORMATIONS OF DIAMONDLIKE CARBON COATINGS UNDER VARIOUS ATMOSPHERES*

J. C. Sánchez-López,[a] A. Erdemir,[b] C. Donnet,[c] and T. C. Rojas[a]

[a]Instituto de Ciencia de Materiales de Sevilla (CSIC-Universidad de Sevilla),
Avda. Américo Vespucio s/n, Isla de la Cartuja, 41092 Sevilla, Spain
[b]Energy Technology Division, Argonne National Laboratory, Argonne, IL 60439 USA
[c]Laboratoire Traitement du Signal et Instrumentation, UMR 5516, Université Jean Monnet,
42023 St-Etienne Cedex 2, France

March 2002

Paper to be presented at International Conference on Metallurgical Coatings and Thin Films, San Diego, CA, April 21-26, 2002.

*Work supported by Spanish MEC and by U.S. Department of Energy, Office of Science, under Contract W-31-109-Eng-38.

FRICTION-INDUCED STRUCTURAL TRANSFORMATIONS OF DIAMONDLIKE CARBON COATINGS UNDER VARIOUS ATMOSPHERES

J. C. Sánchez-López,[a] A. Erdemir,[b] C. Donnet,[c] and T. C. Rojas[a]

[a]Instituto de Ciencia de Materiales de Sevilla (CSIC-Universidad de Sevilla),
Avda. Américo Vespucio s/n, Isla de la Cartuja, 41092 Sevilla, Spain
[b]Energy Technology Division, Argonne National Laboratory, Argonne, IL 60439 USA
[c]Laboratoire Traitement du Signal et Instrumentation, UMR 5516, Université Jean Monnet,
42023 St-Etienne Cedex 2, France

Abstract

The structural transformations that occur in diamondlike carbon coatings with increasing hydrogen content have been investigated by Raman spectroscopy, transmission electron microscopy, electron diffraction, and electron-energy-loss spectroscopy. Friction tests were performed with uncoated steel balls against coated substrates at contact stresses of 1 GPa in ambient air (relative humidity = 30 - 40%), dry air (relative humidity < 1%), and dry nitrogen (< 1%). The lowest friction coefficient ($f < 0.02$) was obtained for the most hydrogenated sample in dry nitrogen, where the formation of a third-body layer was observed on the steel surface. Raman spectra obtained from the counterfaces after sliding in humid and dry air revealed a remarkable increase and narrowing of the "D" and "G" peaks with decreasing humidity. Analysis of peak positions and I(D)/I(G) ratios pointed to an increasing order and an enlargement of the sp^2 clusters under friction. The shape and position of the carbon K-edge spectra for the transfer layer are affected the same way, although evidence of extended graphite layer formation was not observed. Development of these differing trends was correlated with the hydrogen-to-carbon ratio of the gas precursor used during the synthesis and with the type of surrounding atmosphere.

Keywords: DLC, friction, environment, Raman, EELS.

*Corresponding author: Fax: +34-95-4460665

E-mail address: jcslopez@cica.es (J. C. Sánchez-López)

1. INTRODUCTION

The preparation of hard forms of amorphous carbon and hydrogenated amorphous carbon, often known as diamondlike carbon (DLC), has been the object of intense study because of such unique DLC properties as high mechanical strength, chemical inertness, and very attractive friction and wear behavior, which make DLC a good prospect for a wide range of tribological applications [1-4]. Nonetheless, DLC tribological behavior is quite dependent on hydrogen content and on environmental parameters such as humidity and temperature. Hydrogen-free DLC films work best in humid test environments, while hydrogenated DLC provides better performance in dry and inert test environments than in open air [5,6]. At elevated temperatures ($\geq$300ºC), hydrogenated DLC films may gradually turn into graphite and hence wear out quickly [7]. In inert environments, including dry nitrogen and vacuum, friction coefficients can reach either ultralow values (down to 0.01 or less) or high values (>0.5). Donnet and Grill demonstrated by rubbing DLC surfaces in UHV conditions that this behavior can be controlled by the hydrogen content of the film [8].

Recently, Erdemir et al. [9] presented a new procedure for plasma-enhanced chemical vapor deposition (PECVD), based on the generation of hydrogen-rich methane plasmas, that can lead to the formation of DLC films affording friction coefficients as low as 0.003. Further details of this deposition process are provided in earlier works [10-12]. We believe that the high chemical inertness of DLC films is primarily responsible for their generally low friction coefficients. Furthermore, the formation of a carbon-rich transfer layer on surfaces sliding against DLC seems to be essential for further reductions in friction coefficients and for very long wear lives [5,7,12]. The open dangling bonds of the carbon atoms lying on the

surface are largely passivated by the hydrogen atoms present in the films, and the interaction is therefore established between two hydrocarbon polymerlike topcoats through weak van der Waals forces [1]. An electrostatic repulsion is also possible between the hydrogen-terminated sliding surfaces because of the differential electronegativity of the hydrogen and carbon atoms. Such repulsive forces at the sliding counterfaces may counteract the weak van der Waals attractions [13]. In addition, other authors propose a wear-induced graphitization to support the stable and low-friction nature of DLC films [14,15].

In this work, we have used Raman spectroscopy, transmission electron microscopy (TEM), electron diffraction (ED), and electron-energy-loss spectroscopy (EELS) to analyze the microstructures of the transfer layers formed on the steel balls rubbed against DLC films. The information provided by these techniques provided insight into the friction-induced structural modifications at the counterfaces that account for the observed tribological behavior of certain DLC films.

2. EXPERIMENTAL

The DLC films tested in this study were deposited on AISI-H13 steel disks with a room-temperature PECVD process that used either pure C_2H_2, CH_4, or a CH_4/H_2 mixtures as the gas precursor. A tetrahedral amorphous carbon film (hereafter called ta-C) with no hydrogen and high sp^3 character was grown by an arc-PVD process and is included here for comparison. Details of the hydrogenated DLC and hydrogen-free DLC film deposition processes can be found in Refs. 10 and 16. The DLC-coated steel substrates were friction-tested in a ball-on-disk tribometer in various atmospheres (dry nitrogen, dry air , and ambient air) under a 10-N load at a sliding speed of 0.1 m/s for a distance of 500 m. The uncoated AISI52100 steel balls (9.5 mm in diameter) produced a maximum contact Hertzian pressure of 1.04 GPa. A longer friction test was run in dry nitrogen for a sliding distance of 125 km to increase the formation

of debris particles. After reaching the steady-state friction regime, the balls were removed from the tribometer and the structural chemistry of the transfer layers formed on the balls was analyzed by micro-laser Raman, TEM, ED, and EELS techniques.

Raman spectra of the films were measured with a Renishaw Raman microscope employing a HeNe laser at 632.8 nm with an output power of 25 mW focused to a spot size of ≈2 μm. TEM/EELS observations were carried out in a Philips CM200 microscope operating at 200 kV and equipped with a parallel detection EELS spectrometer from Gatan (766-2 kV). The carbon K-edge was recorded in the diffraction mode with a camera length of 700 mm and an entrance aperture of 2 mm. Measured energy resolution at the zero-loss peak of the coupled microscope/spectrometer system was ≈1.4 eV. Spectra were recorded for dark current and channel-to-channel gain variation. Low-loss spectra were also recorded in the same illumination area (≈1 μm in diameter). After subtraction of the background by a standard power-law function, the spectra were deconvoluted for plural scattering with the Fourier-ratio method. All of these treatments were performed within the EL/P program (Gatan).

3. RESULTS AND DISCUSSION

3.1. Frictional properties

The tribological properties of all DLC samples used in our study are summarized in Table I, together with their deposition conditions. The friction coefficients of the DLC films are classified by decreasing hydrogen-to-carbon (H/C) ratios of the source gases from which they were prepared. Attending to the observed friction behavior, the samples can be divided into two groups: (I) Moderate friction in AA, low and stable friction in DN (samples DLC10, DLC6, DLC4); (II) Low friction in AA, high and unsteady in DN (DLC1, ta-C). The lowest and the most stable friction coefficient (0.02) was obtained with the most hydrogenated DLC

film (Group I) in dry nitrogen. The friction behavior of Group II is typical of hydrogen-free DLC films function better in humid environments than in dry and inert atmospheres. The DLC1 film that was prepared from the gas precursor with the lowest hydrogen-to-carbon ratio (C_2H_2) is the film that most closely approaches the behavior of the tetragonal amorphous carbon (ta-C).

Figure 1 depicts a sequence of friction tests performed on the DLC10 coating while the surrounding media was switched from dry nitrogen to ambient or dry air, remaining on the same wear track. From these experiments, the negative influence of both humidity and oxygen on friction is rather obvious, with the coefficient rising from 0.02 to 0.2-0.3, depending on the specific environment. The friction curves obtained in DA are characterized by alternating periods of low friction coefficients with higher values. However, in the DN atmosphere, friction tends to decrease almost immediately down to 0.02 even though very high values were attained in the previous period; this demonstrates the reversibility of the tribological system in affording very low friction values when the chemical inertness of the surrounding media is restored.

3.2 Raman characterization of transfer layer

These macroscopic results are correlated at the microscopic level by differences in transfer layers and wear debris formation processes. Optical examination of the wear scars revealed the transfer of material from the DLC surface to the mating steel balls. Figure 2 presents photomicrographs of the ball surfaces after testing the DLC10 film in the three types of environment, together with their associated Raman spectra. The wear scars formed on the steel balls in the AA and DA tests are characterized by removal of the transfer layer from the contact area and accumulation of debris particles around the edges of the wear scars. Conversely, in the DN environment, no loose powder is seen and the third-body layer appears to be covering the Hertzian contact area. The transfer buildup affects the tribological behavior

of the DLC coatings so that the friction process takes place by interfilm sliding between two distinct films (neither of the original surfaces is in contact) that slide across one another. This transfer layer acts as a lubricant and decreases the friction coefficient to the extremely low observed values [5,7,14].

The Raman spectra obtained from the counterfaces (Fig. 2) are dominated by sharp D and G features of the sp^2 sites of all disordered carbons at 1350 and 1570 cm^{-1}, respectively. The D band arises from the breathing modes of sp^2 atoms in clusters of sixfold aromatic rings [17]. This mode is forbidden in perfect graphite and becomes active only in the presence of disorder. Development of the D peak indicates disordering of graphite but ordering of an amorphous carbon structure; its intensity is proportional to the number and clustering of rings, while its width is more related to a narrower distribution of clusters with different order and dimensions. The G mode of graphite involves the in-plane bond-stretching motion of pairs of carbon sp^2 atom; this mode does not require the presence of sixfold rings, and so it occurs at all sp^2 sites (in aromatic or olefinic chains). Therefore, the main changes affect the position and the width rather than the peak intensity. Decrease of width and peak-shift upward are attributed to a progressive reduction of defects (bond-angle and bond-bending disorder) in the sp^2 amorphous carbon network.

We further evaluated the positions and intensities of the G and D peaks by fitting the components with two Gaussian functions. Compared to the initial spectrum of DLC10 (Fig. 3a), a shift to a higher frequency of the G-peak (1572 up to 1596 cm^{-1}) and a downshift of the D-peak (1378 down to 1326 cm^{-1}), together with a concomitant decrease of their widths, are seen in the sequence AA < DA < DN. These changes can be explained by an increment in number, size, and order of sp^2 aromatic clusters from an initial highly amorphous sp^2-bonded carbon network. The specific environment controls the extent of this ordering process as it

progresses further when access of oxygen or moisture to the surface is restricted by inert-gas molecules. The effects of the surrounding atmosphere on the Raman spectra of the remaining DLC coatings (not shown) result in similar tendency to that observed in the DLC10 sample, although the increase and narrowing of the D and G peaks there is less pronounced because the hydrogen-to-carbon ratio in the DLC10 precursor is lower. The modifications for the hydrogen-free sample (ta-C) differ noticeably from the DLC (H/C) series and will be discussed later separately.

The influence of the initial film microstructure on the sharpening of the G and D peaks is discussed next. In Fig. 3, we show the Raman spectra of the original as-deposited DLC films (Fig. 3a) compared to those obtained after sliding (Fig. 3b) in dry nitrogen. In the original films, the D peak appears as an asymmetric broadening of the G peak toward lower frequencies samples DLC1 and DLC4. The D peak becomes more intense and defined for DLC6 and DLC10 films, for which hydrogen was mixed in the precursor with methane at 50 and 75%, respectively. The I(D)/I(G) ratio after the Gaussian fit is indicated in Fig. 3a;. this ratio increases after development of the D peak. Thus, the use of CH_4/H_2 mixtures to synthesize the DLC films presupposed an effective enlargement of the sp^2 cluster size. The structural transformations induced during the friction test, manifested as an increase and separation of the D and G components, are determined by the initial microstructure of the film. By increasing the hydrogen-to-carbon ratio of the precursor, a higher effective enlargement and ordering of the sp^2 aromatic domains and a significant reduction of friction coefficient at the interface are obtained. Nevertheless, the size of the aromatic cluster must remain below 2 nm. This value is the limit of validity of the Tuinstra and Koening equation [18] for which an inverse dependence of I(D)/I(G) ratio on crystallite size is predicted. Based on this critical value, a proportionality of this parameter to the number and clustering of rings is proposed [17].

Others features observed in the Raman spectra are the presence of a broad peak centered at ≈650-670 cm^{-1} and other smaller bands at lower frequencies. The presence of these peaks was more evident in the less-hydrogenated films (DLC1 and ta-C) tested in ambient air environments, as can be seen in Fig. 4. The origin of these peaks can be attributed to the formation of iron oxide by tribochemical reaction of the uncoated steel ball with the surrounding atmosphere. The positions of the peaks in the range of 225 to 650 cm^{-1} match quite well with those observed in iron oxide phases [19].

Another peculiarity observed in samples DLC1 and ta-C is the appearance of a peak at ≈1330 cm^{-1}; when this peak is present, the intensity of the G band is strongly reduced or practically nonexistent. A single broad peak at 1332 cm^{-1} in the Raman spectrum is a typical signature of the sp^3-bonded diamond phase [20]. The structure of ta-C films is characterized by high sp^3-hybridized carbon and thus when this film in friction-tested in ambient air, that component is clearly observed in the transfer layer. DLC1 has the lowest hydrogen-to-carbon ratio and its tribological behavior is closest to diamondlike. These facts could explain the similarity in friction and Raman behavior between these two samples.

3.3. TEM/EELS characterization of transfer layer

To obtain more knowledge about the structural transformations giving rise to the ultralow friction coefficient under dry nitrogen, we applied TEM, ED, and EELS techniques on the DLC10 coating and the transfer layer formed on the steel ball after sliding in this atmosphere. Figure 5 displays the carbon K-edge energy-loss spectra for the as-deposited DLC10 sample and the transfer layer, together with those of amorphous carbon and graphite specimens for comparison. The main features are the two maxima at ≈285.5 and 295 eV, corresponding to the 1s-π^* and 1s-σ^* transitions, respectively, observed in graphite. However, in comparison with graphite, the original DLC10 coating and its transfer layer do not present the 1s-π^* peak so enhanced and the 1s-σ^* fine structure appears merged. This loss

of long-range order causes a relaxation of the selection rules for transitions and leads to the observed changes. These features are typical of amorphous and nanocrystalline materials, and this is confirmed when comparing the DLC spectra with the spectrum of an amorphous carbon film obtained by evaporation onto a copper grid. Nevertheless, in the transfer layer, the π^* peak becomes more defined. Narrowing of the 1s-π^* transition is believed to be due to a reduction of defects, bond-angle, and bond-bending disorder in the film. These situations generate band-tail and localized states in the gap with excitation energies closer to the threshold. The increasing ordering of the carbon network causes removal of such states and thereby higher definition in the 1s-π^* transition. At the same time, sp^2 carbon atoms bonded to hydrogen may produce a peak between the π^* peak and the edge of the $\sigma*$ band at 287.5 eV, in particular for high hydrogen contents. Hydrogen desorption has been proposed to occur in vacuum during friction [21,22], thus lubricating the surfaces in contact. This phenomenon could affect the structure of the DLC film, leading to formation of C=C bonds and therefore enhancing the intensity of the 1s-π^* transition.

Figure 6 displays TEM photomicrographs and diffraction patterns collected for the as-deposited DLC10 sample and the transfer layer generated in dry nitrogen; diffraction patterns for evaporated amorphous carbon and graphite are included for comparison. The original film has an essentially featureless microstructure (Fig. 6a), confirmed by the presence of strong diffuse rings in the corresponding electron diffraction pattern. Two faint rings can be detected with d-spacing of approximately 2.3 and 1.3 Å, as previously observed in other studies on DLC films [15]. The origin of these rings has been suggested as (110) and (220) diffractions of a short-range diamondlike structure. However, based on the diffraction pattern obtained from an evaporated carbon film (Fig. 6c), these rings can also be assigned to a short-range sp^2 structure. The presence of a larger central spot also points out the overlapping of the strongest (002) graphite reflection from a very disordered sp^2-network. For comparison, the diffraction

pattern of a graphite layer is shown in Fig. 6d. In this case, three clear rings with d-spacing of approximately 3.3, 2.2, and 1.3 Å are visible.

After friction-testing (Fig. 6b), a distribution of particles with sizes of 10 to 50 nm was observed in the microstructure of the transfer layer, although the electron diffraction pattern resembles those of the original film and the evaporated amorphous carbon layer, indicating a very poor crystalline character. The increment in order and size of the sp^2 aromatic clusters observed by Raman spectroscopy on the transfer layer formed in the dry nitrogen atmosphere is not noticeable by electron diffraction. Friction in dry nitrogen may favor less distorted and more ordered sp^2 clusters, but the resulting structure is still very far from that of an extended graphite layer. These results reveal the laser Raman technique as a more suitable characterization tool for following friction-induced structural transformation in small-dimension crystals. Also, laser photon penetration in carbon is restricted to a shallow depth (20-50 nm) and this method is therefore useful for studying near-surface structures of carbon films.

4. CONCLUSIONS

The frictional response of DLC films with increased hydrogen content and prepared by PECVD has been related to the structural transformations detected on counterfaces after friction-testing in various atmospheres. The films prepared with high H/C ratios work better in dry-nitrogen atmospheres (friction coefficient of ≈0.02-0.04), whereas those with little or no hydrogenation provide lower friction values (0.1-0.3) in humid environments. A transfer film is built up on the steel ball surfaces, which suggests a friction mechanism by interfilm sliding and lower shear strength. Chemical characterization by laser Raman spectroscopy of the transfer layers revealed a disordered graphite-like and diamondlike structure in the hydrogenated DLC and t-aC, respectively.

A deeper investigation was performed on the most hydrogenated film in order to elucidate the processes responsible for the ultralow friction coefficients. Structural characterization of the transfer layer by Raman spectroscopy evidenced a simultaneous increase and sharpening of the D and G peaks as the friction coefficient decreased markedly. These structural modifications are related to a progressive ordering of an initial highly disordered sp^2-bonded C network by reduction of defects and clustering of sixfold aromatic rings. The degree of this transformation is favored with the increase of H/C ratio of the gas precursor and the chemical inertness of the surrounding testing atmosphere. Complementary structural characterization by electron diffraction (ED) and transmission electron microscopy (TEM) revealed the essentially amorphous nature of both films (the as-deposited film and the transfer layer), but no additional information could be inferred due to the absence of long-range order. Electron-energy-loss spectroscopy (EELS), however, is sensitive to local coordination in the C structure, and a more resolved 1s-π^* transition was noticed after friction with this technique. This variation pointed out the higher participation of π electrons due to a reduction of defects, bond angle, and bond-bending disorder in the film structure, in agreement with the Raman conclusions.

Based on the tribological behavior and the structural characterization by the Raman, TEM, EELS, and ED techniques, we conclude that the size of the aromatic domains must still be very small (<20 Å) because no typical features of nanocrystalline graphite were observed. Furthermore, graphite does not afford low friction in inert environments as here it is observed in dry nitrogen. Finally, laser Raman spectroscopy has proven to be a very suitable tool for determining friction-induced structural modifications, performing better than electron spectroscopies or diffraction techniques in small-dimension crystals.

ACKNOWLEDGMENT

Funding for this work was provided by Spanish MEC and by the U.S. Department of Energy, Office of Science, under Contract W-31-109-Eng-38.

REFERENCES

1. A. Erdemir and C. Donnet, in B. Bhushan (ed.), Modern Tribology Handbook, CRC Press, Boca Raton, FL, USA, 2000, p. 871.

2. C. Donnet, Surf. Coat. Technol. 100-101 (1998) 180.

3. A. Grill, Surf. Coat. Technol. 94-95 (1997) 507.

4. A. Grill and B. S. Meyerson, in K. E. Spear and J. P. Dismukes (eds.) Synthetic Diamond: Emerging CVD Science and Technology, John Wiley & Sons, New York, 1994, p. 91.

5. J. C. Sánchez-López, C. Donnet, J. Fontaine, M. Belin, A. Grill, V. Patel, and C. Jahnes. Diamond Relat. Mater. 9 (2000) 638.

6. B. K. Tay, D. Sheeja, Y. S. Choong, S. P. Lau, and X. Shi, Diamond Relat. Mater. 9 (2000) 819.

7. K. Holmberg, J. Koskinen, H. Ronkainen, J. Vihersalo, J.P. Hirvonen, and J. Likonen, Diamond Films Technol. 4 (1994) 113.

8. C. Donnet and A. Grill, Surf. Coat. Technol. 94-95 (1997) 456.

9. A. Erdemir, O. L. Erylmaz, I. B. Nilufer, and G. R. Fenske, Surf. Coat. Technol. 133-134 (2000) 448-454.

10. A. Erdemir, G. R. Fenske, J. Terry, and P. Wilbur, Surf. Coat. Technol. 94-95 (1997) 525.

11. A. Erdemir, I. B. Nilufer, O. L. Erylmaz, M. Beschliesser, and G. R. Fenske, Surf. Coat. Technol. 121 (1999) 589.

12. A. Erdemir, O. L. Erylmaz, I. B. Nilufer, and G. R. Fenske, Diamond Relat. Mater. 9 (2000) 632.

13. A. Erdemir, Surf. Coat. Technol. 146-147 (2001) 292.

14. Y. Liu, A. Erdemir, and E. I. Meletis, Surf. Coat. Technol, 94-95 (1997) 463.

15. Y. Liu and E. I. Meletis, J. Mater. Sci. 32 (1997) 3491.

16. R. H. Horsfall, Proc. 41st Annual Technical Conf., Society of Vacuum Coaters, Boston, MA, USA, Society of Vacuum Coaters, Albuquerque, NM, USA, April 18-23, 1998, p. 60.

17. A. C. Ferrari and J. Robertson, Phys. Rev. B 61 (2000) 14095.

18. F. Tuinstra and J. L. Koening, J. Chem. Phys. 53 (1970) 1126.

19. I. R. Beattie and T. R. Gibson, J. Chem. Soc. A 6 (1970) 980.

20. M. H. Grimsditch and A. K. Ramdas, Phys. Rev. B 11 (1975) 3139.

21. T. Le Huu, H. Zaïdi, and D. Paulmier, Wear 181-183 (1995) 766.

22. C. Donnet, J. Fontaine, A. Grill, and T. Le Mogne, Trib. Lett. 9 (2000) 137.

Table I. Growing conditions and friction coefficients under various testing environments for the films studied

Sample	Synthesis	H/C	AA	DN	DA
DLC10	75% H_2 + 10% CH_4	10	0.28	0.02	0.05-0.1
DLC6	50% H_2 + 50% CH_4	6	0.21	0.04	0.25-0.38
DLC4	100% CH_4	4	0.23	0.06	0.5
DLC1	100% C_2H_2	1	0.3	0.8	0.07-0.4
ta-C	arc-PVD	0	0.14	0.6-0.7	0.3-0.7

Figure captions

Fig. 1. Changes in friction coefficient of DLC10 film sliding against uncoated steel ball in a sequence of testing environments (AA: ambient air; DN: dry nitrogen; DA: dry air).

Fig. 2. Photomicrographs of wear scars formed on uncoated steel balls during friction-testing of DLC10 film in AA, DA, and DN atmosphere, together with corresponding Raman spectra.

Fig. 3. Raman spectra of original DLC films (a) compared to those from transfer layer formed on ball counterface after sliding in DN atmosphere (b).

Fig. 4. Raman spectra of least-hydrogenated (DLC1) and free-hydrogen (ta-C) DLC films, as-deposited and after friction tests in ambient air.

Fig. 5. Energy-loss spectra recorded at carbon K-edge in as-deposited DLC10 film and transfer layer in DN. Spectra for an amorphous carbon and graphite film are included for comparison.

Fig. 6. TEM micrograph and associated electron diffraction pattern of the as-deposited DLC10 film (a) compared to those from transfer layer formed under friction in DN (b); also shown are electron diffraction pattern of an evaporated carbon film (c) and graphite (d).

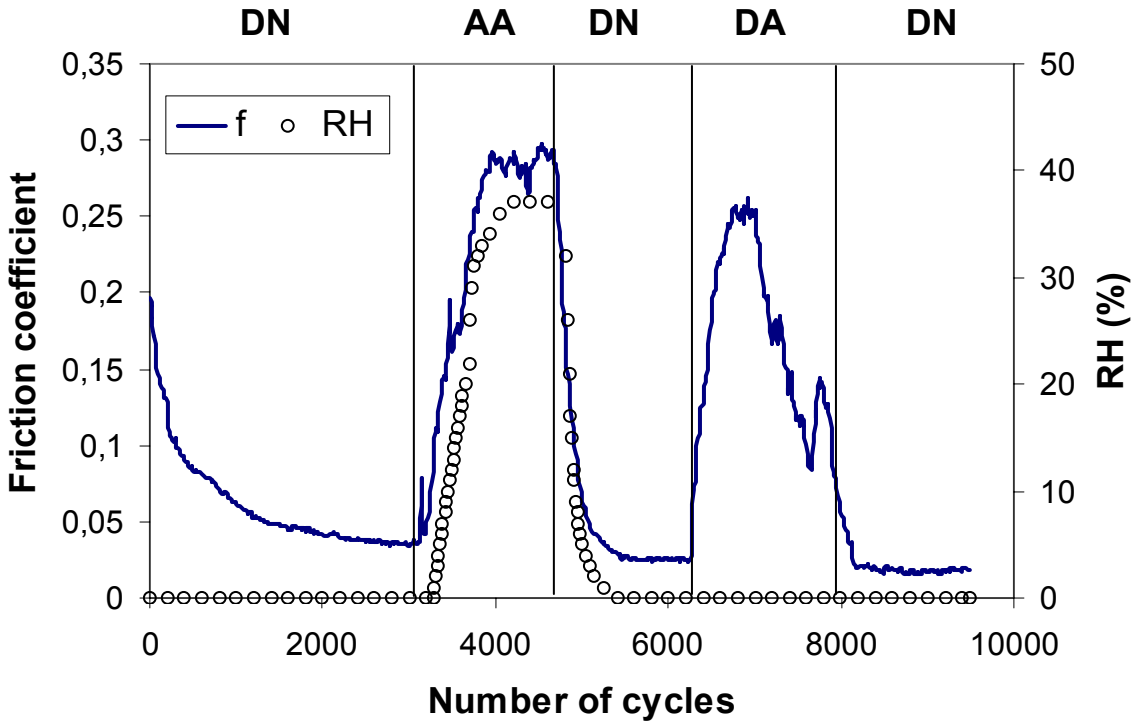
DN
AA
DN
DA
DN
f
RH
Friction coefficient
RH (%)
Number of cycles
0,35
0,3
0,25
0,2
0,15
0,1
0,05
0
50
40
30
20
10
0
0
2000
4000
6000
8000
10000

Fig. 1

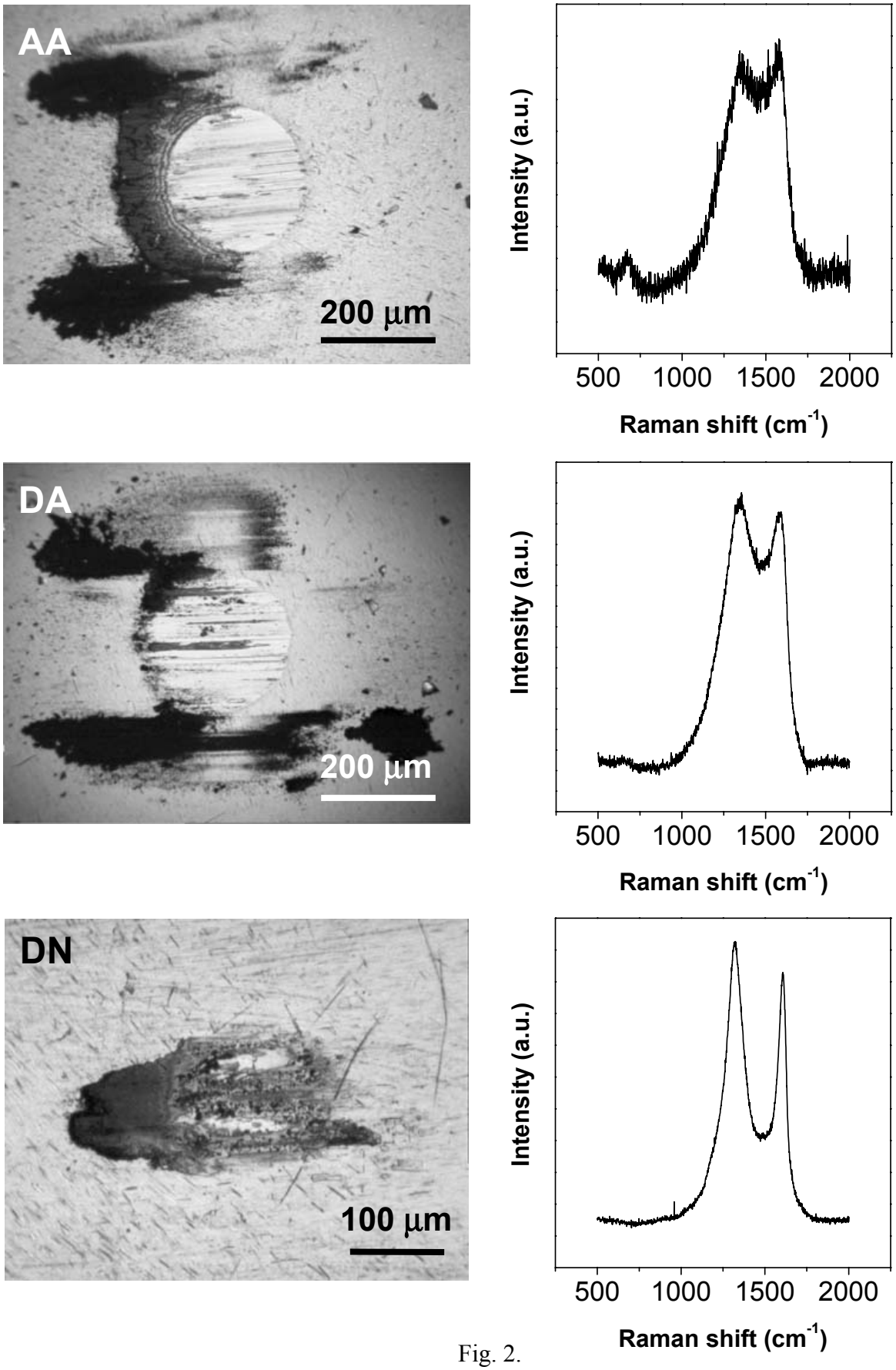
AA
200 μm
Intensity (a.u.)
500
1000
1500
2000
Raman shift (cm-1)
DA
200 μm
Intensity (a.u.)
500
1000
1500
2000
Raman shift (cm-1)
DN
100 μm
Intensity (a.u.)
500
1000
1500
2000
Raman shift (cm-1)

Fig. 2.

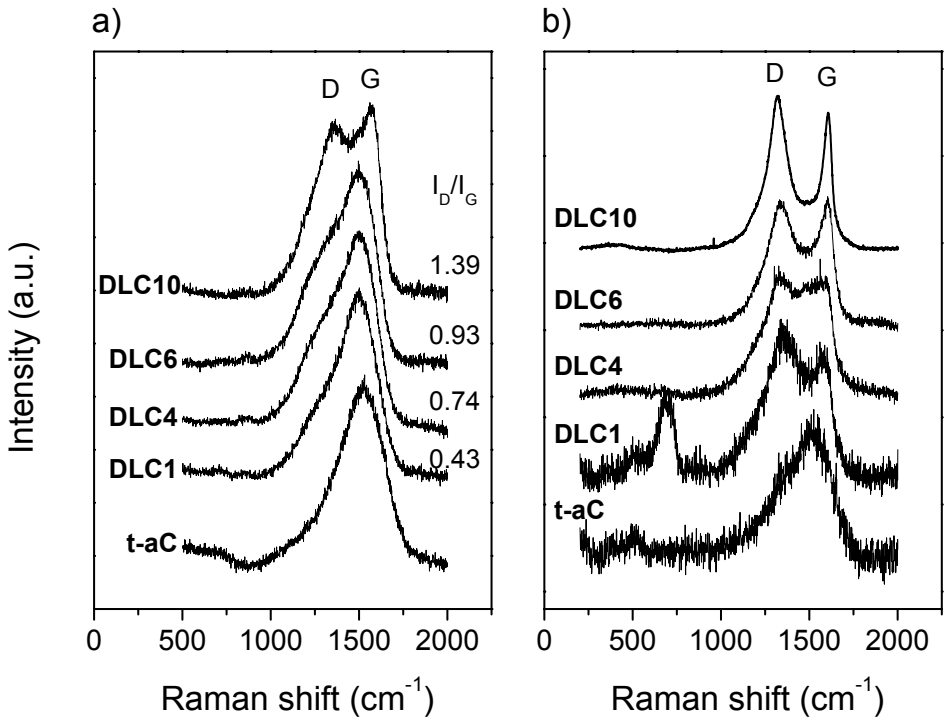
a)
b)
D
G
I_D/I_G
DLC10
1.39
DLC6
0.93
DLC4
0.74
DLC1
0.43
t-aC
Intensity (a.u.)
0
500
1000
1500
2000
Raman shift (cm^{-1})

Fig. 3.

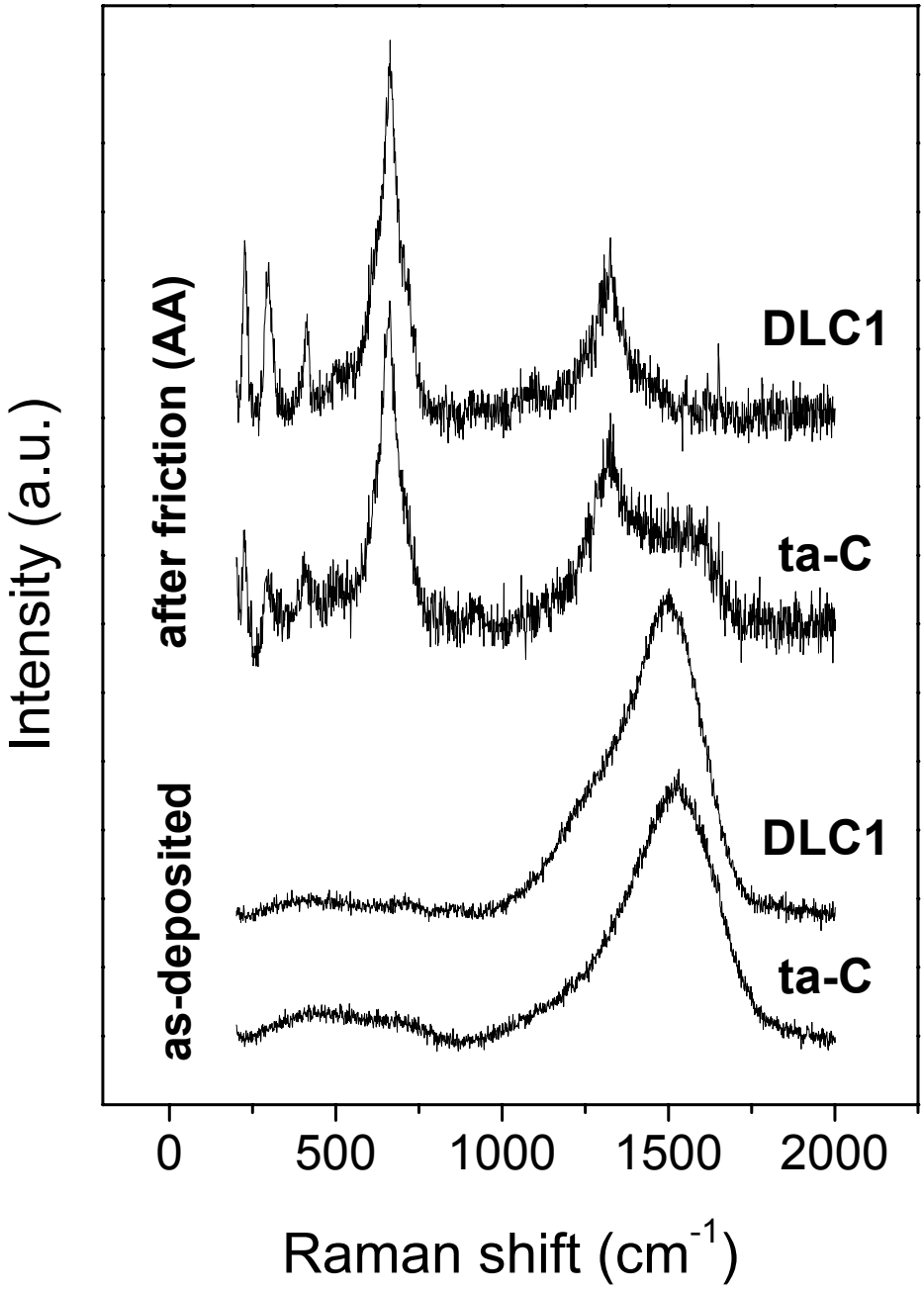
Intensity (a.u.)
after friction (AA)
DLC1
ta-C
as-deposited
DLC1
ta-C
0
500
1000
1500
2000
Raman shift (cm-1)

Fig. 4.

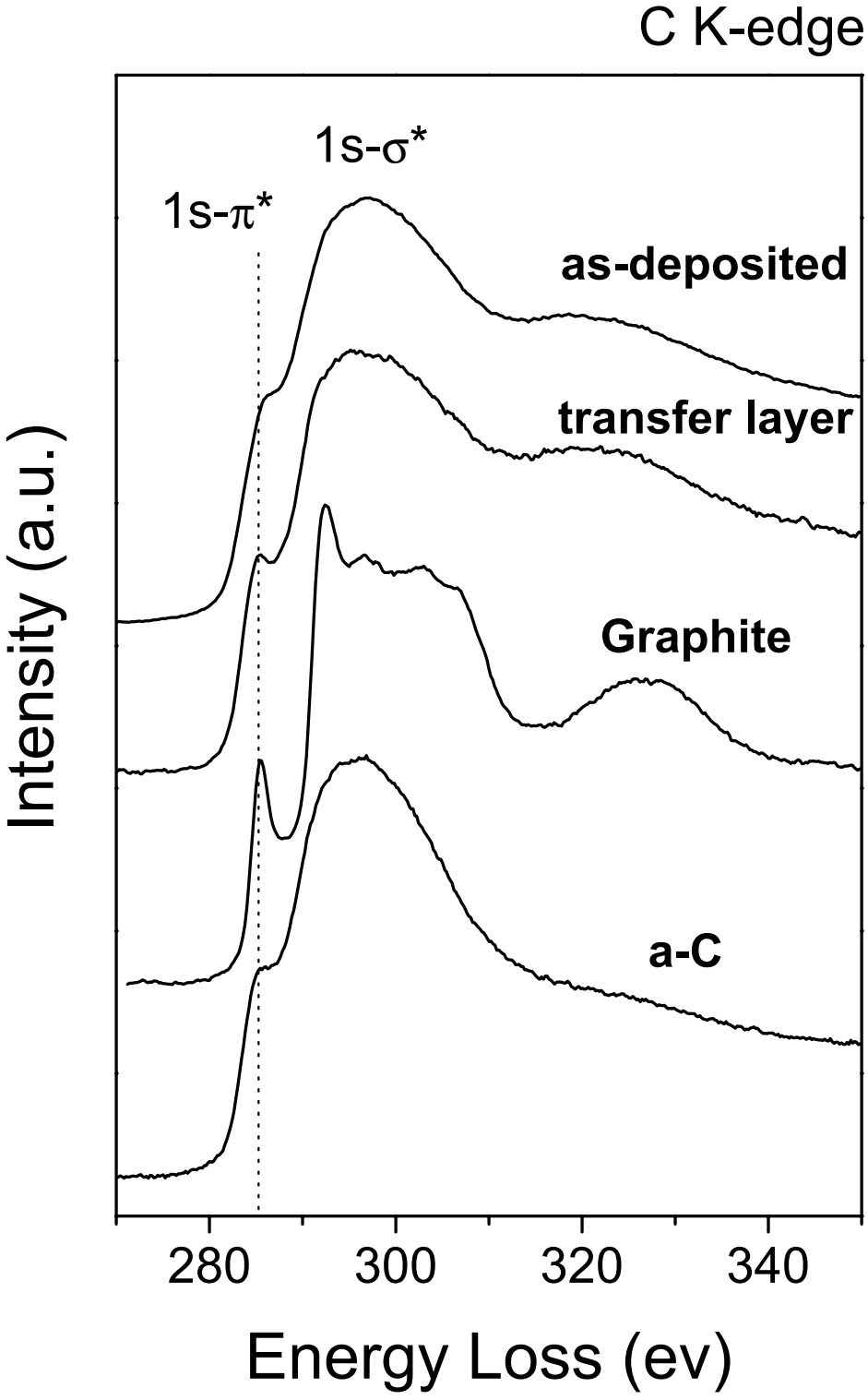
C K-edge
1s-σ*
1s-π*
as-deposited
transfer layer
Graphite
a-C
Intensity (a.u.)
280
300
320
340
Energy Loss (ev)

Fig. 5

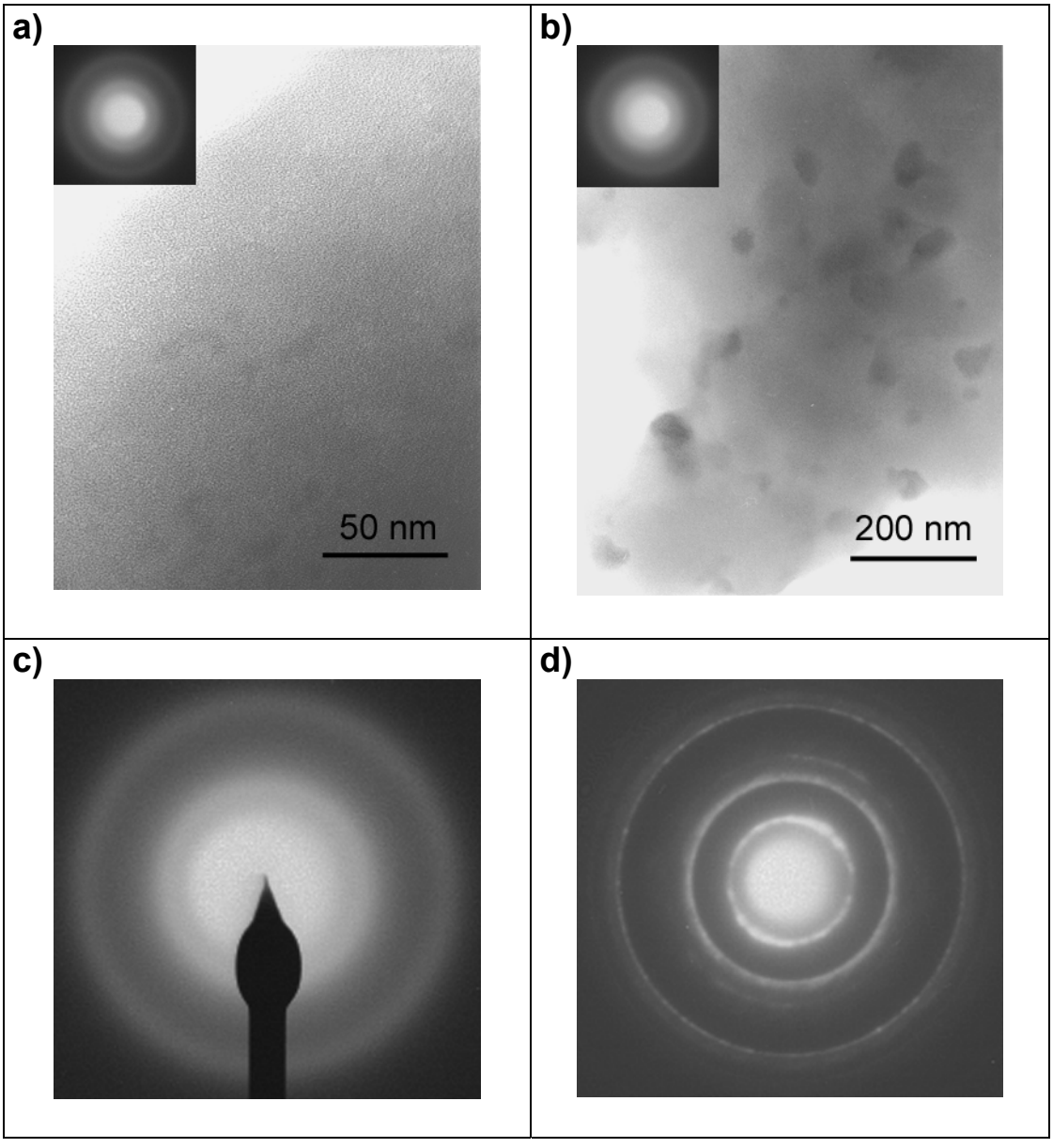

Fig. 6